DOI: 10.1002/ejic.200700121

Synthesis, Characterization and Stability of Spirodiene Complexes of Molybdenum(II): New Route to *ansa*-Molybdenocene and Ring-Functionalized Molybdenocene Compounds

Jan Honzíček,[a] Filipe A. Almeida Paz,[b] and Carlos C. Romão*[a]

Keywords: Metallocenes / Molybdenum / Spiro compounds / Functionalized cyclopentadienes / X-ray diffraction

The reactions of $[Mo(CO)_2(Cp)(NCCH_3)_2][BF_4]$ (**1**) with spiro[2.4]hepta-4,6-diene and spiro[4.4]nona-1,3-diene give the complexes $[Mo\{\eta^4\text{-}C_5H_4(CH_2)_2\}(CO)_2(Cp)][BF_4]$ (**3**) and $[Mo\{\eta^4\text{-}C_5H_4(CH_2)_4\}(CO)_2(Cp)][BF_4]$ (**4**), respectively. $[Mo\{\eta^4\text{-}C_5H_4(CH_2)_2\}(CO)_2(Cp)][BF_4]$ (**3**) is stable towards ring opening at room temperature, but its formation is accompanied by small amounts of ring-opening products $[Mo(\eta^5\text{-}C_5H_4CH_2\text{-}\eta^1\text{-}CH_2)(CO)(Cp)][BF_4]$ (**5**) and $[Mo\{\eta^5\text{-}C_5H_4(CH_2)_2\text{-}\eta^1\text{-}CO\}(CO)(Cp)][BF_4]$ (**6**). With 1,1-dimethylspiro[2.4]hepta-4,6-diene, two isomers with the formula $[Mo\{\eta^4\text{-}C_5H_4CH_2C(CH_3)_2\}(CO)_2(Cp)][BF_4]$ are formed (**7** and **8**). While the *endo*-isomer **7** is stable towards ring opening, the *exo*-isomer **8** slowly rearranges to the ring-opened product $[Mo\{\eta^5\text{-}C_5H_4C(CH_3)_2CH_2\text{-}\eta^1\text{-}CO\}(CO)(Cp)][BF_4]$ (**9**). The reaction of $[Mo(CO)_2(Ind)(NCCH_3)_2][BF_4]$ (**2**) with spiro[4.4]nona-1,3-diene also gives the diene coordinated species $[Mo\{\eta^4\text{-}C_5H_4(CH_2)_4\}(CO)_2(Ind)][BF_4]$ (**11**), which is the first example of a structurally characterized, coordinated, unsubstituted spirodiene. In contrast, reaction of **2** with spiro[2.4]hepta-4,6-diene leads directly to the *ansa*-cyclopentadienyl complex $[Mo(\eta^5\text{-}C_5H_4CH_2\text{-}\eta^1\text{-}CH_2)(CO)(Ind)][BF_4]$ (**12**). Reaction of **12** with bromine or iodine leads to the formation of Cp-substituted molybdenocene derivatives $[Mo\{\eta^5\text{-}C_5H_4(CH_2)_2X\}(CO)(Ind)X][BF_4]$ (**13**: X = Br, **14**: X = I). The compounds $[Mo(\eta^5\text{-}C_5H_4CH_2\text{-}\eta^1\text{-}CH_2)(CO)(Ind)][BF_4]$ (**12**) and $[MoBr\{\eta^5\text{-}C_5H_4(CH_2)_2Br\}(CO)(Ind)][Br]\cdot 0.5H_2O$ (**13a**) were structurally characterized, and they open the way to new functionalized molybdenocene complexes that have biological applications.

Introduction

Bent metallocene complexes of the type $[M(Cp)_2X_2]$ (M = Ti, V, Nb, Mo; X = halide) have been investigated for their use in biological applications ever since their antitumor activity was discovered by Köpf and Köpf-Maier.[1] Because of the particular requirements of such applications, which include aqueous solubility and biocompatibility, considerable attention has been given in the last few years to the synthesis of modified and functionalized variants of such complexes. Substitution of halide ligands gives compounds with modified physical and chemical properties. This approach leaves the "$M(Cp)_2$" moiety unchanged, and properly chosen substituents can help in overcoming problems, such as low water solubility[2] or biological incompatibility,[3] that complicate the use of the parent compounds. Furthermore, substitution can protect the "$M(Cp)_2$" moiety during transport into the tumor cells. The active species is then generated in close proximity of or directly in the tumor cell.[4]

However, modification of the Cp rings seems to be a more promising approach towards solving of the abovementioned problems, as shown by the many results obtained in the field of bioorganometallic radiopharmaceuticals.[5] Such a modification could enable the fine tuning of cytostatic properties as was recently shown by the titanocene compounds.[6] Moreover, it allows the introduction of reactive groups that offer an anchor on which to append biologically active molecules capable of directing the final complex to the target receptors or diseased tissues.[7] This is a central issue in chemotherapy, because the treatment then becomes more effective at low doses and the damage to non-targeted and/or healthy tissues is minimized.

In the case of group IV metallocenes, a variety of ring-substituted compounds containing functional groups on one or both cyclopentadienyl rings is known,[8] thus supporting a wider range of in vitro[9] and in vivo biological tests.[10] For group V and VI metals, the quest for suitable synthetic routes is still on-going. Following our long-standing interest in the chemistry of the highly stable molybdenocene fragment, and the fact that the dichloride $[MoCl_2(Cp)_2]$ is currently under comprehensive scrutiny because of its mechanism towards antitumor action,[11] we decided to

[a] Instituto de Tecnologia Química e Biológica da Universidade Nova de Lisboa,
Av. da República, EAN, 2780-157 Oeiras, Portugal
[b] Department of Chemistry, University of Aveiro, CICECO, 3810-193 Aveiro, Portugal
Fax: +351-21-441-12-77
E-mail: ccr@itqb.unl.pt

Supporting information for this article is available on the WWW under http://www.eurjic.org or from the author.

explore a new suitable approach towards achieving functionalization of its rings. The introduction of alkyl substituents in one[12] or both rings has been documented.[13]

Compounds with η^5:η^1-cyclopentadienidoethyl ligands, which are derived from C–C cleavage of spirodiene compounds by the Mo^0 species, are potent precursors for ring-functionalized group VI metallocenes.[14] When Mo atoms are used for this purpose, the resulting *ansa* complex $[Mo(\eta^5\text{-}C_5H_4CH_2\text{-}\eta^1\text{-}CH_2)_2]$ enables the introduction of various substituents containing functional groups onto the cyclopentadienyl rings.[15] The resulting products are functionalized equally on both rings. The problem of functionalizing only one of cyclopentadienyl rings could probably be solved by the use of the *ansa* compound $[Mo(\eta^5\text{-}C_5H_4CH_2\text{-}\eta^1\text{-}CH_2)(\eta^4\text{-}C_5H_6)(CO)]$[16] that was previously synthesized from $[Mo(\eta^5\text{-}C_5H_4CH_2\text{-}\eta^1\text{-}CH_2)(CO)_3]$[17] and cyclopentadiene through a photochemical route. Unfortunately, none of these routes is very practical in the absence of metal vapor synthesis equipment or sound control of the photochemical reactions. In the present work, we propose another approach starting from the readily available Mo^{II} allyl complexes $[Mo(\eta^3\text{-}C_3H_5)(CO)_2(Cp')]$ (Cp′ = Cp, Ind). These compounds, activated by HBF_4, as well as their stabilized counterparts $[M(CO)_2(Cp')(NCCH_3)_2][BF_4]$ (**1**: Cp′ = Cp, **2**: Cp′ = Ind) are known as strong dienophiles that could be capable of coordinating spiro[2.4]hepta-4,6-diene and spiro[4.4]nona-1,3-diene to give the η^4-diene complexes.[18] The question to be answered involved the possibility that such a coordination could activate the spirodiene ligands towards C–C cleavage and aromatization of the cyclopentadienyl ring, even in spite of the fact that the Mo center is in the +2 oxidation state; this issue was probed before, not only for Mo, but also for W, Fe, Co and Ni.[19] The following work gives an affirmative answer to this question and provides a new route to differentially substituted molybdenocene derivatives.

Results

Cyclopentadienyl Complexes

$[Mo(CO)_2(Cp)(NCCH_3)_2][BF_4]$ (**1**) reacts with spiro[2.4]-hepta-4,6-diene and spiro[4.4]nona-1,3-diene in CH_2Cl_2 at room temperature to give compounds $[Mo\{\eta^4\text{-}C_5H_4(CH_2)_2\}(CO)_2(Cp)][BF_4]$ (**3**) and $[Mo\{\eta^4\text{-}C_5H_4(CH_2)_4\}(CO)_2(Cp)][BF_4]$ (**4**), respectively. While **4** was the only product detected in its reaction mixture, for the reaction leading to **3**, two other ring-opening products were detected in the crude product. The sample collected before recrystallization contained approximately 86% of compound **3**, 7% of $[Mo(\eta^5\text{-}C_5H_4CH_2\text{-}\eta^1\text{-}CH_2)(CO)(Cp)][BF_4]$ (**5**) and 7% of $[Mo\{\eta^5\text{-}C_5H_4(CH_2)_2\text{-}\eta^1\text{-}CO\}(CO)(Cp)][BF_4]$ (**6**), as determined by ^1H NMR spectroscopy (see Scheme 1).

Both **3** and **4** are stable complexes in solution in the absence of strong light, and they can be recrystallized from CH_2Cl_2/Et_2O. This means that compounds **5** and **6** are not formed directly by decomposition of **3** but result from unclear events occurring in the initial reaction mixture. The infrared spectra of compounds **3** and **4** show two CO stretching vibrations each in the typical region for similar cationic compounds with terminal carbonyl groups (**3**: 2019, 1960 cm^{-1}; **4**: 2020, 1964 cm^{-1}).[19] ^{1}NMR and $^{13}C\{^1H\}$ NMR spectra of these compounds are consistent with the η^4-coordination of the appropriate spirodiene. The resonances for the protons of the diene system are shifted to higher field upon coordination, relative to the resonances for the free ligands. Furthermore, coordination results in nonequivalent methylene groups. In the NMR spectrum of compound **3**, the signals for the protons of both methylene groups are also shifted to higher field. Nevertheless, this shift is much smaller than that recently reported for the iron(0) complex $[Fe\{\eta^4\text{-}C_5H_4(CH_2)_2\}(CO)_3]$[20] (see Table 1). We assign the resonance at higher field to the methylene protons on the external face of the coordinated spiro[2.4]hepta-4,6-diene, in accord with reported literature observations for coordinated cyclopentadienes. In fact, $[M(\eta^4\text{-}5R,5R'\text{-}C_5H_4)L_n]$ complexes, where R, R′ = CH_2X, systematically reveal higher field resonances for the CH_2X substituent on the diene face opposite to the metal.[21] This effect is also observed in the very similar complexes $[M\{\eta^4\text{-}C_5(CH_3)_5H\}(CO)_2(Cp)]^+$ (M = Mo, W).[12a]

In compound **4**, only the protons of the methylene groups that are in neighborhood of the *ipso* carbon atom are affected by the coordination. The signals that are shifted to higher field are assigned to the methylene protons on the external face, while the signals at lower field to those on

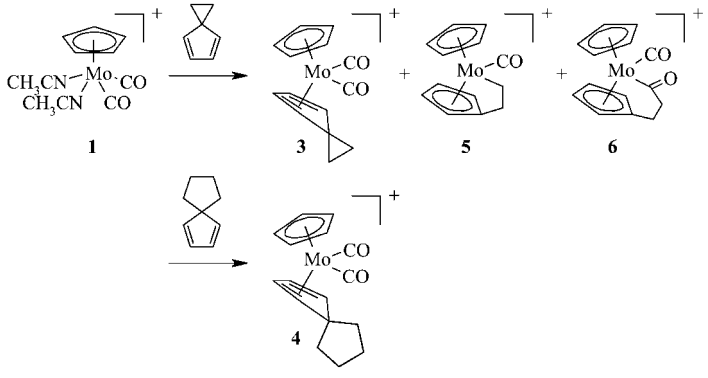

Scheme 1. Products of the reactions between compound **1** and spiro[2.4]hepta-4,6-diene and spiro[4.4]nona-1,3-diene.

Table 1. Chemical shifts of spiro[2.4]hepta-4,6-diene, spiro[4.4]nona-1,3-diene, and their complexes [ppm].

		C_5H_4	C_{ipso}	CH_2	CH_2
Spiro[2.4]hepta-4,6-diene[14b]	^1H	6.54, 6.15		1.68	
	$^{13}C\{^1H\}$	139.2, 129.1	37.7	12.5	
$[Mo\{\eta^4\text{-}C_5H_4(CH_2)_2\}(CO)_2(Cp)][BF_4]$ (**3**)	^1H	6.49, 4.82		1.32,[a] 0.66[b]	
	$^{13}C\{^1H\}$	96.8, 88.7	—[c]	28.6,[a] 14.3[b]	
$[Fe\{\eta^4\text{-}C_5H_4(CH_2)_2\}(CO)_3]$[20]	^1H	5.73, 2.90		0.90,[a] 0.32[b]	
Spiro[4.4]nona-1,3-diene	^1H	6.34, 6.22		1.89	1.72
	$^{13}C\{^1H\}$	144.0, 128.8	43.6	32.5	26.1
$[Mo\{\eta^4\text{-}C_5H_4(CH_2)_4\}(CO)_2(Cp)][BF_4]$ (**4**)	^1H	6.13, 5.09		2.09,[a] 1.31[b]	1.70,[a] 1.60[b]
	$^{13}C\{^1H\}$	96.4, 85.7	72.4	52.3,[a] 37.8[b]	25.3,[a] 25.0[b]
$[Mo\{\eta^4\text{-}C_5H_4(CH_2)_4\}(CO)_2(Ind)][BF_4]$ (**11**)	^1H	5.30, 4.85		1.83,[a] 1.10[b]	1.57,[a] 1.44[b]
	$^{13}C\{^1H\}$	93.2, 85.2	71.6	51.9,[a] 37.1[b]	24.9,[a] 24.7[b]

[a] Internal face. [b] External face. [c] Not observed.

the internal face. The connectivity between the methylene groups was established by selective irradiation experiments. $^{13}C\{^1H\}$ NMR spectra of compounds **3** and **4** show that the signals for the diene carbon atoms are shifted to higher field, while the signals for the *ipso* carbon atoms and for the neighboring methylene groups appear at lower field (see Table 1). The methylene carbon atoms on the external face have resonances that are upfield relative to those for the carbon atoms on the internal face.

The ring-opening products **5** and **6** were not possible to isolate and identify separately. They were identified by NMR spectroscopy, performed on the reaction mixture containing **5** and **6** together with **3**, and their identification was based on the diastereotopic protons of the methylene groups. The connectivity between the assigned multiplets of these minor compounds was established by selective irradiation experiments (for appropriate spectra see the Supporting Information). For compound **5**, these resonances were found at δ = 2.82, 2.62, –0.41 and –0.89 ppm. The last two high field signals were assigned to the methylene group bonded to molybdenum as depicted in Scheme 1. They are in agreement with those reported for similar *ansa* alkyls such as $[Mo(\eta^5\text{-}C_5H_4CH_2\text{-}\eta^1\text{-}CH_2)_2]$.[14a] Compound **6** exhibits multiplets in its NMR spectrum at δ = 3.57–3.37 ppm (10 lines) and δ = 2.48–2.28 ppm (10 lines). These values are very similar to those reported for the compound that results from the ring opening of $[Fe\{\eta^4\text{-}C_5H_4(CH_2)_2\}(CO)_3]$ to form $[Fe(\eta^5\text{-}C_5H_4CH_2CH_2\text{-}\eta^1\text{-}CO)(CO)_2]$, which has the same kind of metal–acyl ligation proposed for **6**: δ = 3.40 (t); 2.15 ppm (t).[20] The presence of the acyl ligand could not be unequivocally established by solution IR spectroscopy because of the interference from moisture-derived absorptions and because of the low concentration of the compound. In KBr pellets, the mixture decomposed quickly.

The effect of the presence of substituents on the sp^3 carbon atoms of the spirodiene was studied by using 1,1-dimethyl-spiro[2.4]hepta-4,6-diene. This diene reacts with compound **1** in CH_2Cl_2 at room temperature (16 h) to give a 1:1:1 mixture of the *endo* **7** and *exo* isomers **8** of $[Mo\{\eta^4\text{-}C_5H_4CH_2C(CH_3)_2\}(CO)_2(Cp)][BF_4]$ and a ring-opened product (Scheme 2). The ^1H NMR spectra of **7** and **8** show signals for the protons in the Cp and spirodiene rings with chemical shifts similar to those found for compound **3**. Relative to the uncoordinated ligand, the resonances for the methyl protons of the *exo* isomer (**8**) and the methylene protons of the *endo* isomer (**7**) appear at higher field (**8**: δ = 0.90 ppm; **7**: δ = 0.48 ppm), which leads to the structural

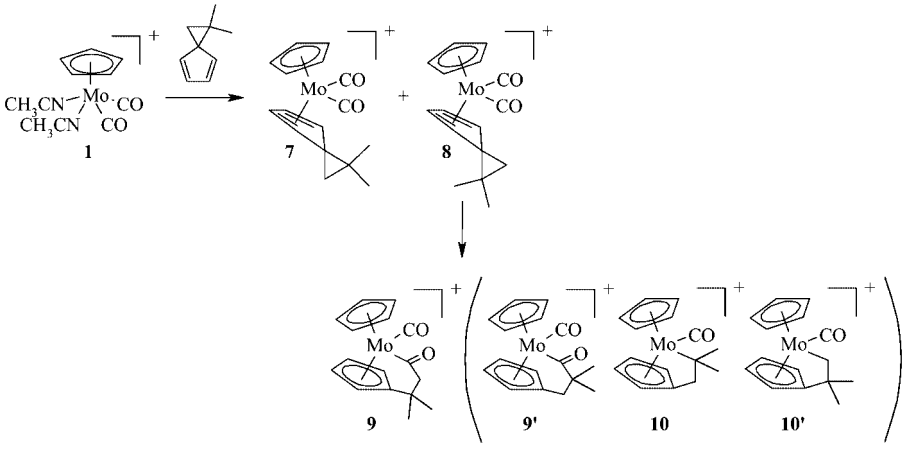

Scheme 2. Reaction of compound **1** with 1,1-dimethyl-spiro[2.4]hepta-4,6-diene.

assignment in Scheme 2.[21] The methyl groups of compound **7**, which are on the internal face, are not affected by coordination.

^{1}H NMR measurements of the 1:1:1 mixture in CD_2Cl_2, after 12 and 24 h, show exclusive activation of the *exo* isomer **8** towards ring opening (see Scheme 2). In fact, at room temperature, the resonances belonging to **7** remain unaffected, while **8** converts into a new compound, which may have one of the structures **9**, **9′**, **10**, or **10′**, as depicted in Scheme 2. The mixture of compounds **7** and the new compound, which was obtained after stirring for 24 h in CH_2Cl_2, is stable at room temperature, and the relative abundance of both components remains unchanged. No evidence for the formation of a second ring-opening product was observed. We were unable to isolate this new compound from the reaction mixture. Therefore, its tentative characterization relies upon the NMR spectroscopic data since solution IR spectroscopy could not conclusively identify an acyl function.

In agreement with the proposed strained *ansa* structure that would be expected from the chemistry of coordinatively activated spirodienes already exemplified by compounds **5** and **6**, the ^{1}H NMR spectrum of the new compound shows diastereotopic methylene and methyl groups. The chemical shift for the methylene protons (δ = 2.22–2.12 ppm) rules out structure **10′**, since the Mo–CH_2 signal should appear at a much higher field. Structure **10** is not clearly compatible with the available ^{1}H NMR spectroscopic data for related compounds. In fact, the CH_2 group at the Cp ring appears at ca. 2.5 ppm in compounds such as [Mo(η^5-$C_5H_4CH_2$-η^1-CH_2)$_2$][15] or in **12** (see below). The more open, alternative acyl-bridged structures present the resonances for C_5H_4–CH_2 at $\delta > 3$ ppm in well-established compounds such as [Fe(η^5-$C_5H_4CH_2CH_2$-η^1-CO)(CO)$_2$] (ca. 3.4 ppm)[20] or the related [Mo(η^5-$C_5H_4CH_2CH_2X)_2X_2$] (X = Cl, Br, I, SPh; ca. 3.5 ppm).[15] Such chemical shift values are in agreement with those in compound **6**, which has two methylene resonances at δ = 2.22–2.12 ppm and δ = 3.57–3.37 ppm. However, since the new compound does not have any resonances in the δ = 3.5 ppm region, the formation of structure **9′** is most unlikely. Therefore, the NMR spectroscopic data is most compatible with structure **9**, although no definitive assignment is possible at present. This structure corresponds to the opening of the unhindered face of the spirodiene C_3 ring, which is facing the metal.

Indenyl Compounds

[Mo(CO)$_2$(Ind)(NCCH$_3$)$_2$][BF$_4$] (**2**) was used as a starting material for the synthesis of mixed–ring molybdenocenes containing indenyl rings. Its reaction with spiro[4.4]-nona-1,3-diene gave [Mo{η^4-$C_5H_4(CH_2)_4$}(CO)$_2$(Ind)][BF$_4$] (**11**) in high yield (Scheme 3). The IR and NMR spectra of **11** are similar to those of its cyclopentadienyl counterpart **4**. In the NMR spectra of compound **11**, the signals for the spiro[4.4]nona-1,3-diene protons and carbon atoms are shifted to a higher field than those of **4**, which is in according with the higher electrophilicity of the Mo^{II} center. The CO stretching vibrations of **11** occur at 2005 and 1950 cm^{-1}. These values are lower than those of the cyclopentadienyl counterpart **4**. The structure of **11** was confirmed by X-ray diffraction crystallography, as discussed below.

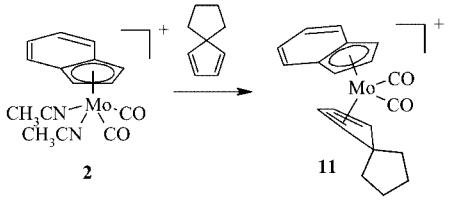

Scheme 3. Synthesis of compound **11**.

In contrast to the latter reaction, the ring-opened *ansa* compound [Mo(η^5-$C_5H_4CH_2$-η^1-CH_2)(CO)(Ind)][BF$_4$] (**12**) was found to be the sole product of the reaction between **2** and spiro[2.4]hepta-4,6-diene (Scheme 4). The IR spectrum of this compound shows only one band in range for CO vibrations (1991 cm^{-1}). The ^{1}H NMR spectrum shows four multiplets that are assigned to the substituted cyclopentadienyl ring, seven multiplets for the indenyl ring, and four multiplets for the ethylene bridge. The nonequivalence of the cyclopentadienyl and indenyl protons, which is caused by the low symmetry of complex **12**, is also observed in the ^{13}C{^{1}H} NMR spectrum. The methylene protons were found to be diastereotopic, which is similar to that found for the cyclopentadienyl analog **5**. The abnormally high-field signal in the ^{1}H NMR (δ = –0.07 ppm and –3.21 ppm) and ^{13}C{^{1}H} NMR (δ = –39.3 ppm) spectra provide evidence for the bonding of the methylene group to the metal. The structural assignment of **12** was confirmed by X-ray crystallography, as discussed below.

Compound **12** is a suitable starting material for the preparation of ring-substituted compounds. Indeed, according to Scheme 4, its reactions with halogens give the compounds [Mo{η^5-$C_5H_4(CH_2)_2X$}(CO)(Ind)X][BF$_4$] (**13**: X = Br, **14**: X = I) in high yield. These compounds provide NMR spectra that are expected for compounds with η^5-bonded indenyl and substituted η^5-cyclopentadienyl rings. In compound **13**, the protons of the methylene group bonded to the cyclopentadienyl ring are diastereotopic and

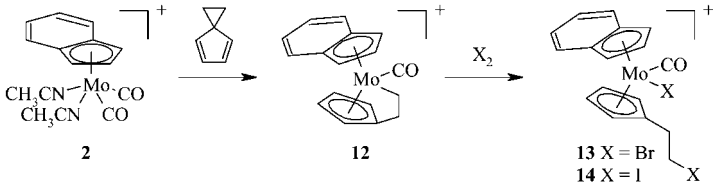

Scheme 4. Reaction of compound **2** with spiro[2.4]hepta-4,6-diene.

thus give rise to a six-line multiplet at δ = 3.54 ppm. In the case of compound **14**, this effect was observed for both methylene groups. The six-line multiplets are found at δ = 3.37 and 2.84 ppm. This effect is probably caused by the larger steric hindrance of iodine. The IR spectra of compounds **13** and **14** show CO stretching vibrations at 2055 and 2049 cm^{-1}. These values correspond to those found for analogous compounds without substituents on the cyclopentadienyl ring.[12a] These structural assignments are supported by the X-ray diffraction crystal structure obtained for compound **13**, as discussed below.

Mass Spectrometry

Compounds **3**, **4**, **11**, **12**, **13**, and **14** were characterized by positive-ion ESI mass spectrometry. These compounds have common features and give the peaks for the parent cation $[M - BF_4]^+$ and for $[M - BF_4 - CO]^+$. As expected, the peaks for $[M - BF_4 - 2(CO)]^+$ were observed for compounds containing two carbonyl ligands (**3**, **11**). The mass spectra for the spirodiene compounds **3** and **11** and the *ansa* compound **12** contain peaks that are formed from dehydrogenation. Compounds **3** and **12** exhibit the peaks assigned to $[M - BF_4 - 2(CO) - H_2]^+$ and $[M - BF_4 - CO - H_2]^+$ in their spectra, respectively. The peaks for $[M - BF_4 - 2(CO) - H_2]^+$ and $[M - BF_4 - 2(CO) - 2H_2]^+$, which were found in the case of compound **11**, suggest the possibility of single and double dehydrogenation for the compounds that contain a chain of four methylene groups.

X-ray Analyses of Compounds 11, 12, and 13a

The structures of $[Mo\{\eta^4\text{-}C_5H_4(CH_2)_4\}(CO)_2(Ind)][BF_4]$ (**11**), $[Mo(\eta^5\text{-}C_5H_4CH_2\text{-}\eta^1\text{-}CH_2)(CO)(Ind)][BF_4]$ (**12**), and $[MoBr\{\eta^5\text{-}C_5H_4(CH_2)_2Br\}(CO)(Ind)][Br]\cdot 0.5H_2O$ (**13a**) were determined in the solid state at 100(2) K (**11**) or at 150(2) K (**12**, **13a**) by single-crystal X-ray diffraction. Figures 1, 2, and 3 depict the crystallographically independent cationic complexes present in the crystal structures of **11**, **12**, and **13a**, respectively. Tables 2, 3, and 4 summarize the most relevant and structurally significant geometrical parameters associated with these structures. The asymmetric units of **12** and **13a** each comprise two crystallographically independent molybdenum complexes (Figures 2 and 3).

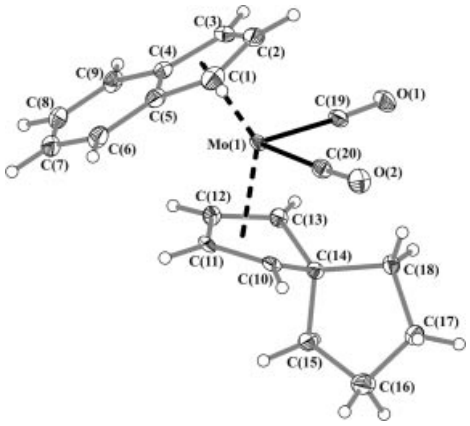

Figure 1. Schematic representation of the cationic complex $[Mo\{\eta^4\text{-}C_5H_4(CH_2)_4\}(CO)_2(Ind)]^+$ present in the crystal structure of **11**; the labeling scheme for all non-hydrogen atoms is shown. Thermal ellipsoids are drawn at the 30% probability level, and hydrogen atoms are represented as small spheres with arbitrary radii. Mo–C bonds to the η^5-indenyl and $\eta^4\text{-}C_5H_4(CH_2)_4$ organic ligands are shown as black-filled dashed bonds to the corresponding centers of gravity ($C_{g,Ind}$ and $C_{g,diene}$, respectively).

The Mo–C bonds observed for the indenyl ligands [found in the ranges 2.301(5)–2.413(4) Å, 2.254(4)–2.460(3) Å, and 2.264(3)–2.454(3) Å for structures **11**, **12**, and **13a**, respectively] are well within the range found for similar structures (38 entries in the CSD, with Mo···C interatomic distances in the range 2.24–2.50 Å; median 2.31 Å).[22] The significant spread of the interatomic Mo···C distances (magnitude of 0.26 Å for the expected range) is typical for η^5-Ind coordination. Likewise, the distances to the center of gravity, Mo···$C_{g,Ind}$, are in perfect agreement with known values for η^5-hapticity (38 entries; 1.95–2.19 Å with a median of

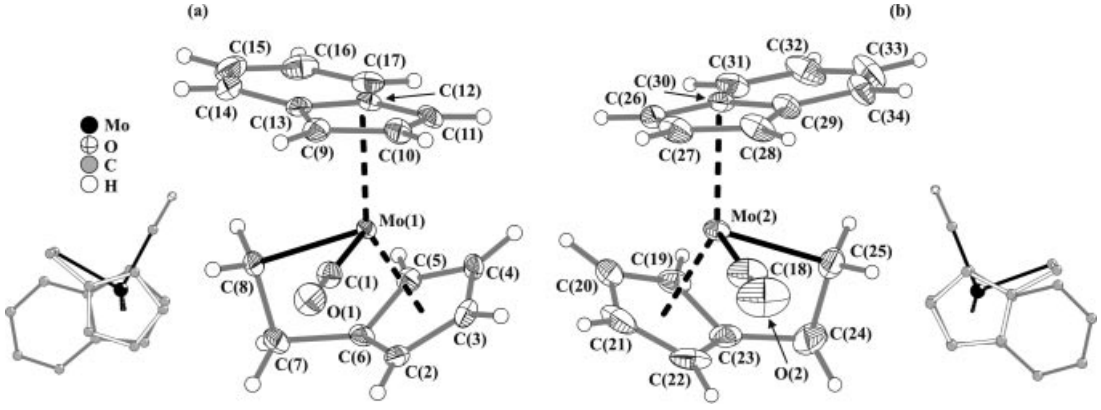

Figure 2. Schematic representation of the two crystallographically independent $[Mo(\eta^5\text{-}C_5H_4CH_2\text{-}\eta^1\text{-}CH_2)(CO)(Ind)]^+$ cationic complexes present in the crystal structure of **12** (*R* and *S* configurations); the labeling scheme for all non-hydrogen atoms is shown. Thermal ellipsoids are drawn at the 30% probability level, and hydrogen atoms are represented as small spheres with arbitrary radii. Mo–C bonds to the η^5-indenyl and η^5-cyclopentadienyl ligands are shown as black-filled dashed bonds to the corresponding centers of gravity ($C_{g,Ind}$ and $C_{g,Cp}$, respectively). The top view of each complex is represented on the side (hydrogen atoms have been omitted for clarity).

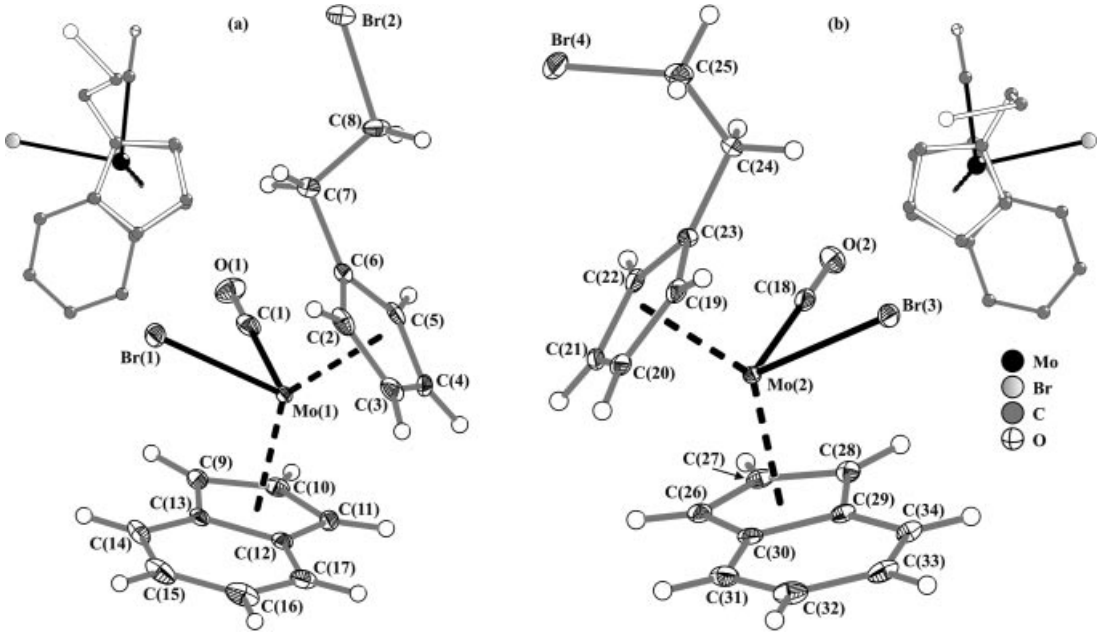

Figure 3. Schematic representation of the two crystallographically independent $[MoBr\{\eta^5\text{-}C_5H_4(CH_2)_2Br\}(CO)(Ind)]^+$ cationic complexes present in the crystal structure of **13a** (*S* and *R* configurations); the labeling scheme for all non-hydrogen atoms are shown. Thermal ellipsoids are drawn at the 30% probability level, and hydrogen atoms are represented as small spheres with arbitrary radii. Mo–C bonds to the η^5-indenyl and η^5-cyclopentadienyl ligands are shown as black-filled dashed bonds to the corresponding centers of gravity ($C_{g,Ind}$ and $C_{g,Cp}$, respectively). The top views of each complex are represented on the side (hydrogen atoms have been omitted for clarity).

Table 2. Selected bond lengths [Å] and angles [°] for the molybdenum coordination environment present in $[Mo\{\eta^4\text{-}C_5H_4(CH_2)_4\}(CO)_2(Ind)][BF_4]$ (**11**).[a,b]

Mo(1)–C(1)	2.301(5)	$C_{g,Ind}$···Mo(1)–C(19)	113.63(4)
Mo(1)–C(2)	2.276(5)	$C_{g,Ind}$···Mo(1)–C(20)	112.45(5)
Mo(1)–C(3)	2.304(4)	$C_{g,Ind}$···Mo(1)···$C_{g,diene}$	137.03(5)
Mo(1)–C(4)	2.414(4)	$C_{g,diene}$···Mo(1)–C(19)	97.28(4)
Mo(1)–C(5)	2.413(4)	$C_{g,diene}$···Mo(1)–C(20)	98.78(4)
Mo(1)–C(10)	2.448(4)	C(19)–Mo(1)–C(20)	84.96(18)
Mo(1)–C(11)	2.276(4)		
Mo(1)–C(12)	2.284(4)		
Mo(1)–C(13)	2.446(4)		
Mo(1)–C(19)	1.975(5)		
Mo(1)–C(20)	1.968(4)		
Mo(1)···$C_{g,Ind}$	2.002(2)		
Mo(1)···$C_{g,diene}$	2.062(2)		

[a] $C_{g,Ind}$ – centroid of the coordinated η^5-indenyl aromatic ring [C(1) to C(5)]. [b] $C_{g,diene}$ – centroid of the coordinated η^4-diene ligand [C(10) to C(13)].

Table 3. Selected bond lengths [Å] and angles [°] for the two molybdenum coordination environments present in $[Mo(\eta^5\text{-}C_5H_4CH_2\text{-}\eta^1\text{-}CH_2)(CO)(Ind)][BF_4]$ (**12**, see Figure 2).[a,b]

Complex (a)		Complex (b)	
Mo(1)–C(1)	2.002(3)	Mo(2)–C(18)	1.973(4)
Mo(1)–C(2)	2.297(3)	Mo(2)–C(19)	2.276(4)
Mo(1)–C(3)	2.291(3)	Mo(2)–C(20)	2.290(4)
Mo(1)–C(4)	2.289(3)	Mo(2)–C(21)	2.295(4)
Mo(1)–C(5)	2.276(3)	Mo(2)–C(22)	2.284(4)
Mo(1)–C(6)	2.293(3)	Mo(2)–C(23)	2.303(4)
Mo(1)–C(8)	2.271(3)	Mo(2)–C(25)	2.273(4)
Mo(1)–C(9)	2.307(3)	Mo(2)–C(26)	2.254(4)
Mo(1)–C(10)	2.274(3)	Mo(2)–C(27)	2.275(4)
Mo(1)–C(11)	2.268(3)	Mo(2)–C(28)	2.322(3)
Mo(1)–C(12)	2.377(3)	Mo(2)–C(29)	2.460(3)
Mo(1)–C(13)	2.449(3)	Mo(2)–C(30)	2.375(3)
Mo(1)···$C_{g,Ind}$	1.995(1)	Mo(2)···$C_{g,Ind}$	2.000(1)
Mo(1)···$C_{g,Cp}$	1.944(1)	Mo(2)···$C_{g,Cp}$	1.950(1)
$C_{g,Ind}$···Mo(1)–C(1)	102.81(2)	$C_{g,Ind}$···Mo(2)–C(18)	102.41(2)
$C_{g,Ind}$···Mo(1)–C(8)	108.31(1)	$C_{g,Ind}$···Mo(2)–C(25)	107.90(4)
$C_{g,Ind}$···Mo(1)···$C_{g,Cp}$	145.43(2)	$C_{g,Ind}$···Mo(2)···$C_{g,Cp}$	145.46(2)
$C_{g,Cp}$···Mo(1)–C(1)	105.36(3)	$C_{g,Cp}$···Mo(2)–C(18)	105.24(1)
$C_{g,Cp}$···Mo(1)–C(8)	92.13(1)	$C_{g,Cp}$···Mo(2)–C(25)	91.31(2)
C(1)–Mo(1)–C(8)	88.51(14)	C(18)–Mo(2)–C(25)	92.4(2)

[a] $C_{g,Ind}$ – centroid of the coordinated η^5-indenyl aromatic rings [C(9) to C(13) and C(26) to C(30)]. [b] $C_{g,Cp}$ – centroid of the coordinated η^5-cyclopentadienyl ligand [C(2) to C(6) and C(19) to C(23)].

2.03 Å). The values of the fold angle ψ (3.79° for **11**, 4.41° and 4.63° for **12**, and 5.66° and 6.17° for **13a**) are also in line with this coordination mode (typically in the range 0.25–9.63° with a median of 4.40°).[23]

To the best of our knowledge, complex **11** represents the first reported crystal structure of a complex with an unsubstituted spirocyclic cyclopentadiene group. Spiro[4.4]nona-1,3-diene is coordinated in a typical η^4-coordination fashion (Figure 1), with all Mo···C distances in the range 2.276(4)–2.448(4) Å (Table 2). The corresponding four carbon atoms [C(10) to C(13)] lie almost on the same plane (maximum deviation 0.004(5) Å). This plane is perpendicular to the metal–diene centroid vector [{Mo(1)–$C_{g,diene}$}–P_{diene} = 89.8(3)°; P_{diene} is the diene plane]. The C–C bond lengths of the diene system [C(10)–C(11) = 1.402(7) Å; C(11)–C(12) = 1.424(6) Å; C(12)–C(13) = 1.396(7) Å] correspond to a butadiene fragment. The distance between the centroid of the diene system and molybdenum [$C_{g,diene}$–Mo(1)] is 2.062(5) Å. The spiro carbon atom [C(14)] is found to lie 0.496(4) Å out of the diene plane. The angle

Table 4. Selected bond lengths [Å] and angles [°] for the two molybdenum coordination environments present in [MoBr{η^5-$C_5H_4(CH_2)_2Br$}(CO)(Ind)][Br]·0.5H_2O (**13a**, see Figure 3).[a,b]

Complex (a)		Complex (b)	
Mo(1)–C(1)	2.019(4)	Mo(2)–C(18)	2.005(4)
Mo(1)–C(2)	2.347(3)	Mo(2)–C(19)	2.350(3)
Mo(1)–C(3)	2.369(4)	Mo(2)–C(20)	2.379(3)
Mo(1)–C(4)	2.322(3)	Mo(2)–C(22)	2.283(3)
Mo(1)–C(5)	2.288(3)	Mo(2)–C(21)	2.316(3)
Mo(1)–C(6)	2.289(3)	Mo(2)–C(23)	2.284(3)
Mo(1)–C(9)	2.264(3)	Mo(2)–C(26)	2.291(3)
Mo(1)–C(10)	2.269(3)	Mo(2)–C(27)	2.265(3)
Mo(1)–C(11)	2.308(3)	Mo(2)–C(28)	2.271(3)
Mo(1)–C(12)	2.434(3)	Mo(2)–C(29)	2.454(3)
Mo(1)–C(13)	2.443(3)	Mo(2)–C(30)	2.426(3)
Mo(1)–Br(1)	2.6077(5)	Mo(2)–Br(3)	2.6147(4)
Mo(1)···$C_{g,Ind}$	2.006(1)	Mo(2)···$C_{g,Ind}$	2.002(1)
Mo(1)···$C_{g,Cp}$	1.988(1)	Mo(2)···$C_{g,Cp}$	1.985(1)
$C_{g,Ind}$···Mo(1)–C(1)	103.95(2)	$C_{g,Ind}$···Mo(2)–C(18)	103.82(2)
$C_{g,Ind}$···Mo(1)–Br(1)	107.44(2)	$C_{g,Ind}$···Mo(2)–Br(3)	107.52(2)
$C_{g,Ind}$···Mo(1)···$C_{g,Cp}$	136.79(2)	$C_{g,Ind}$···Mo(2)···$C_{g,Cp}$	136.41(2)
$C_{g,Cp}$···Mo(1)–C(1)	105.00(1)	$C_{g,Cp}$···Mo(2)–C(18)	104.77(1)
$C_{g,Cp}$···Mo(1)–Br(1)	106.60(1)	$C_{g,Cp}$···Mo(2)–Br(3)	107.12(1)
C(1)–Mo(1)–Br(1)	84.59(11)	C(18)–Mo(2)–Br(3)	85.00(10)

[a] $C_{g,Ind}$ – centroid of the coordinated η^5-indenyl aromatic ring [C(9) to C(13) and C(26) to C(30)]. [b] $C_{g,Cp}$ – centroid of the coordinated η^5-cyclopentadienyl ligand [C(2) to C(6) and C(19) to C(23)].

between the diene plane and the plane defined by atoms C10, C13 and C14 [29.3(4)°] is smaller than that previously reported for the spirocyclic isodicyclopentadiene complex of iron(0) [36.2(3)°].[24]

The η^4-bonded spiro[4.4]nona-1,3-diene ligand is found in the less common (*exo*) conformation. So far, nine other structures (from 35 entries available in the CSD) that present the "M(Cp′)(η^4-diene)LL′" (Cp′ = Cp, Cp*, Ind; M = transition metal) moiety display a similar conformation.[22]

By taking into consideration the centers of gravity of the carbon atoms connected to the molybdenum atom in **11** ($C_{g,Ind}$ and $C_{g,diene}$ for the η^5-indenyl and η^4-spiro[4.4]nona-1,3-diene molecules, respectively), we note that the Mo coordination resembles a highly distorted tetrahedron (Figure 1) in which the tetrahedral angles are significantly distorted from the ideal values and range from 84.96(18)° to 137.03(5)° (Table 2). The large angle is subtended between the centers of gravity of the C1–C5 and C10–C13 rings. The two Mo–C≡O bonds form a rather small tetrahedral angle of 84.96(18)°.

A peculiar feature of the structures of both **12** and **13a** is the presence of two crystallographically independent cationic complexes composing the asymmetric unit. As depicted in Figures 2 and 3, the two single complexes belonging to each structure are almost mirror images of each other, with only subtle differences. The slightly distinct bond lengths and angles for each pair of identical complexes are, presumably, a consequence of distinct interactions arising from the crystal packing. When viewed from above (schematic representations on the sides of Figures 2 and 3), the spatial distribution of the aromatic five-membered rings (substituted Cp versus indenyl) is not exactly identical for each pair: while in the one complex the rings are almost eclipsed (dihedral angles of about 3.9° and 1.7° for **12** and **13a**, respectively), in the other complex the substituted cyclopentadienyl ring is slightly rotated towards a staggered conformation (dihedral angles of about 14.3° and 7.5° for **12** and **13a**, respectively).

On the other hand, differences within each pair of identical complexes also arise from the intrinsic conformational flexibility associated with the aliphatic chains. This feature is particularly evident for structure **13a**, in which the two pendant arms of the substituted η^5-C_5H_4 rings have markedly distinct conformations and the angles between the planes containing the two aromatic rings are statistically distinct (ca. 42.0° and 44.1° for the complexes on the left and right, respectively; see Figure 3).

The two substituted cyclopentadienyl ligands of structures **12** and **13a** interact in different manners with the molybdenum centers, basically as a result of their distinct pendant arms. However, both are connected to the metallic center through the cyclopentadienyl ring, which exhibits a typical η^5-coordination fashion. The Mo···C distances for **12** and **13a** are in the ranges 2.284(4)–2.303(4) Å and 2.283(3)–2.379(3) Å, respectively, (Tables 3 and 4), which is in accord with those found from a systematic search in the CSD[22] (1628 entries for η^5-Cp: Mo–C bonds in the range 2.12–2.65 Å with median of 2.33 Å). The cyclopentadienidoethyl (C_5H_4–CH_2–CH_2) ligand is connected to the metallic center in **12** through the η^5-C_5H_4 ring and through the terminal η^1-CH_2 to form a *pseudo*-five-membered chelate ring (Figure 2) with an average bite angle of about 91.7° (Table 3). This value is in good agreement with those reported for the only other two related structures that contain this organic moiety found in the literature (average bite angle of 91.3°).[25] The (2-bromoethyl)cyclopentadienide (C_5H_4–CH_2–CH_2–Br) ligand in **13a** is exclusively bound to the molybdenum center through the η^5-C_5H_4 aromatic ring. A literature search reveals only one other structure that has a ligand of the type C_5H_4–CH_2–CH_2–X (where "X" is a halogen) bound to molybdenum: [Mo(η^5-$C_5H_4CH_2CH_2I)_2$-I_2].[25a]

Interestingly, each crystallographically independent molybdenum center in **12** and **13a** can also be envisaged as being coordinated to four distinct moieties, which renders it as a chiral crystallographic center: in Figure 2 (structure **12**), the depicted complexes have *R* and *S* configurations (left and right, respectively), while in Figure 3 (structure **13a**), the configurations are instead *S* and *R* (left and right, respectively). It is also important to emphasize that these two crystal structures are not ideal crystal racemates, because the two geometrical isomers are not exact mirror images as previously described. Relative to **11**, the tetrahedral coordination geometries of the molybdenum centers in **12** and **13a** are significantly more distorted; while for **12**, the tetrahedral bond lengths and angles are within the ranges 1.944(1)–2.273(4) Å and 88.51(14)–145.46(2)°, respectively, for **13a**, the values are instead in the ranges 1.985(1)–2.6147(4) Å and 84.59(11)–136.79(2)°. Noteworthy is the fact that the larger tetrahedral angles for **13a** (correspond-

ing to the angle between the two centers of gravity of the organic moieties) are comparable to those of **11**; on the other hand, the angles that are >145° for structure **12** (see Table 3) essentially arise as a result of the geometrical constraints imposed by the five-membered chelate rings of the η^5:η^1-cyclopentadienidoethyl ligand.

The crystal packing arrangements of **12** and **13a** are essentially mediated by a considerable number of weak C–H···(O,F,Br) hydrogen bonds (not shown). In structure **13a**, and similarly to that in **11**, π–π interactions between η^5-indenyl organic ligands that belong to neighboring complexes also occur, and the water molecule of crystallization present in the crystal structure is further engaged in two strong and rather liner O–H···Br hydrogen-bonding interactions with two neighboring bromide anions (not shown): O(1 W)–H(1A)···Br(6) with $d_{D\cdots A}$ = 3.292(3) Å and ∠(DHA) = 170(3)°; O(1 W)–H(1B)···Br(5) with $d_{D\cdots A}$ = 3.268(3) Å and ∠(DHA) = 169(4)°.

Discussion

Earlier reports on the reactivity of Mo^0 compounds towards spirodienes include both very reactive Mo atoms[14a] and $Mo(CO)_3(NCCH_3)_3$.[17] In both cases, the only products observed result from the opening of the cycloalkane ring and concomitant formation of one η^5-C_5H_4–Mo and one η^1-C–Mo bond. Similar reactivity was observed for hexamethylcyclopentadiene $C_5(CH_3)_6$, which reacts with molybdenum metal in the gas phase to give $Mo(CH_3)_2(Cp^*)_2$.[26] This formal C–C oxidative addition reaction is supported by the aromatization of the C_5 ring.

In the present case, the cationic Mo^{II} compounds **1** and **2** are more discriminate in their reactions towards the opening of coordinated spirodienes. The less-strained spiro[4.4]-nona-1,3-diene does not undergo ring opening upon coordination to $[Mo(CO)_2(Cp')]^+$ (Cp′ = Cp, Ind), and the spirodiene complexes **4** and **11** are formed in good yield. These species are stable, and no signs of ring opening were observed. The breaking of the C–C bond takes effect only in the case of the more-strained cyclopropane ring of spiro[2.4]hepta-4,6-diene coordinated to both $[Mo(CO)_2(Cp')]^+$ fragments, but under different circumstances. Reaction of **1** with spiro[2.4]hepta-4,6-diene gives the η^4-diene compound **3** and the *ansa* compounds **5** and **6**. The last two compounds were obtained in a 1:1 molar ratio and result from ring opening of the C_3 ring. Each one represents a type of ring-opening product already described in the literature. In **5**, one CO group is lost and a new C–Mo bond is formed, while in **6**, the broken ring binds to a coordinated CO group instead, which results in an acyl complex. However, **5** and **6** are not formed directly from **3**. In fact, in CH_2Cl_2 solution and under normal laboratory light, **3** remains unchanged for at least 24 h, which is longer than the reaction time for the formation of **3**, **5**, and **6** from **1** and the spirodiene. Irradiation of a clean solution of **3** does not lead to **5**, **6**, or any tractable product. Therefore, the ring opening reaction leading to **5** and **6** takes place through pathways that are not yet clear. In contrast, the indenyl compound **2** does not form a stable or observable diene complex with spiro[2.4]hepta-4,6-diene and gives the *ansa* compound **12** selectively. Our interpretation of the above findings is depicted in Scheme 5.

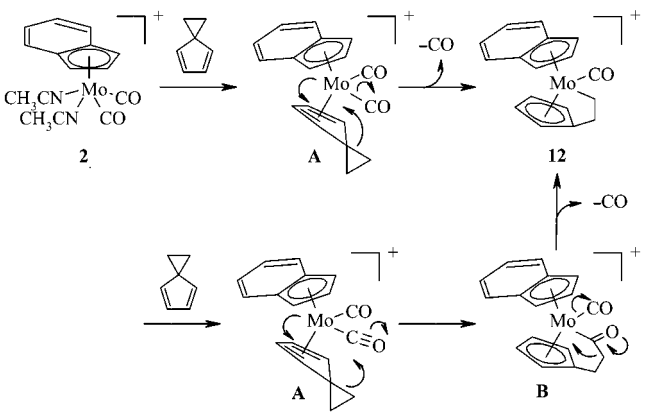

Scheme 5. Proposed pathways to compound **12** (intermediates **A** and **B** were not observed).

In both cases, a diene species should be obtained by substitution of the labile CH_3CN ligands. The dienophilic character of the fragment $[Mo(CO)_2(Cp')]^+$ supports this reasoning. However, once formed, such diene complexes may have a different reactivity, which depends on the Cp′ ring present. In the case where Cp′ = Cp, complex **3** remains stable. In the case where Cp′ = Ind, the putative intermediate **A** (not observed) is expected to be much more labile towards CO loss than **3**. This is in line with the reported higher lability of $[Mo(\eta^4\text{-}C_5H_6)(CO)_2(Ind)]^+$ towards CO loss and formation of $[Mo(CO)(Cp)H(Ind)]^+$ relative to its Cp counterpart.[12a] Therefore, when intermediate **A** loses CO, the facing C–C bond of the C_3 ring adds across to form **12**. The alternative hypothesis that **A** undergoes C–C bond addition to CO to form **B** (not observed), which then looses CO and undergoes CO deinsertion from the acyl to lead to **12** also needs to be considered.[27] These insertion/deinsertion reactions are usually slow at the Cp_2Mo fragment, but they might be favored by the indenyl over the cyclopentadienyl counterpart.

It is interesting to also note the comparison between the reactivity of spiro[2.4]hepta-4,6-diene and 1,1-dimethylspiro[2.4]hepta-4,6-diene towards the fragment $[Mo(CO)_2(Cp)]^+$. The effects of such substituents have been investigated both in coordination-assisted ring opening[28] and in the reduction of the free spiro[2.4]hepta-4,6-dienes.[29] Both substituted and unsubstituted spiro[2.4]hepta-4,6-dienes form η^4 complexes with $[Mo(CO)_2(Cp)]^+$, namely **3**, **7** and **8**. However, while **3** and **7** are stable towards subsequent ring opening, **8** slowly rearranges to a new compound. Although we have not yet been able to identify the structure of this compound, the fact that **8** reacts must mean that the substituted spirodiene is more reactive than its unsubstituted counterpart. In addition, its coordination mode also determines its reactivity, as **7** does not evolve into any ring-opening product. Since **8** has the less-hindered C–C bond

facing the metal, steric factors would favor the formation of **9** (or **10′** for that matter), as is most likely according to the NMR spectroscopic data available. With this view, **10′** would also have been a favorable outcome, but it was not observed. This stereochemical line of reasoning was first encountered for the reaction of 1,1-dimethyl-spiro[2.4]-hepta-4,6-diene[28] and 1-phenyl-spiro[2.4]hepta-4,6-diene[30] with $[Mo(CO)_3(NCCH_3)_3]$, which always led to the opening of the unsubstituted C_{ipso}–CH_2 bond of the C_3 ring. This was interpreted as the result of the preferred coordination of the substituted spirodienes having the substituents on the face opposite to the $Mo(CO)_3$ fragment, as found in **8**.[28] However, the same report reveals that for $Fe_2(CO)_9$ no such clear regioselectivity was observed, which implies that electronic factors may overrule steric considerations, as observed in the chemistry of free spirodienes. Moreover, this stereochemical argument cannot explain the selectivity that prevents the formation of **10′**. Further experimental studies supported by DFT calculations, aiming at the full characterization of the product **9** (or **10**), and the study of the activation of 1,1-dimethyl-spiro[2.4]hepta-4,6-diene by the more reactive $[Mo(CO)_2(Ind)]^+$ fragment are currently underway in our laboratories to try to understand these mechanistic details.

Regardless of the mechanistic questions, the results described mark an important step in our development of ring-functionalized molybdenocene complexes. The transformation of **12** into **13** and **14** follows the pattern previously shown by the groups of Green[14a] and Royo.[14b] The pendant bromo- and iodoalkyl substituents allow the introduction of a wide variety of functions and of bioactive molecules, as ample literature precedent has already shown. A related manipulation starting from **9** (or any of its congeners in Scheme 2) can be envisaged, thus extending the range of compounds to the bis(cyclopentadienyl)molybdenum fragment.

Conclusions and Outlook

Spiro[2,4]hepta-4,6-dienes and spiro[2,4]nona-4,6-diene coordinate readily, to form the products in high yields, to the $[Mo(CO)_2(Cp')]^+$ fragment (Cp′ = Cp, Ind). For the Cp derivatives, ring opening only takes place with the 1,1-dimethyl-spiro[2,4]hepta-4,6-diene. In contrast, the indenyl containing fragment induces a high-yield ring opening of the unsubstituted spiro[2,4]hepta-4,6-diene, but not of spiro[2,4]nona-4,6-diene, to produce the *ansa* compound **12** from which haloalkyl-functionalized fragments are introduced onto a molybdenocene structural framework, as in compounds **13** and **14**. These are among the few examples of ring-functionalized molybdenocene derivatives capable of being manipulated for conjugation with bioactive molecules for biological and medical applications and are the first to contain differentially substituted rings. The preparation of such conjugates is presently underway and is directed towards their use as antitumor drugs.

Experimental Section

Methods and Materials: All operations were performed under nitrogen by using conventional Schlenk-line techniques. The solvents were purified and dried by standard methods.[31] Spiro[2.4]hepta-4,6-diene,[14b] spiro[4.4]nona-1,3-diene,[32] 1,1-dimethyl-spiro[2.4]-hepta-4,6-diene,[33] $[Mo(CO)_2(Cp)(NCCH_3)_2][BF_4]$ (**1**),[34] and $[Mo(CO)_2(Ind)(NCCH_3)_2][BF_4]$ (**2**)[12a] were prepared according to literature procedures. Bromine and iodine (Aldrich) were used as obtained without further purification.

Measurements: Positive-ion electrospray ionization (ESI) mass spectra were recorded with API-ION TRAP (PO 03 MS). Samples were measured in CH_2Cl_2 solution. The molybdenum-containing ions had a clearly visible metal isotope pattern, which arises from the distribution: ^{92}Mo 14.84%, ^{94}Mo 9.25%, ^{95}Mo 15.92%, ^{96}Mo 16.68%, ^{97}Mo 9.55%, ^{98}Mo 24.13%, ^{100}Mo 9.63%.[35] Spectra obtained were computer simulated (WSearch32 2005). Mass peaks listed refer to fragments with the isotopes ^{1}H, ^{12}C, ^{16}O, ^{79}Br, ^{98}Mo, and ^{127}I. ^{1}H and ^{13}C{^{1}H} NMR spectra were recorded in solutions at room temperature with Bruker AMX-300 spectrometer. $CDCl_3$, CD_2Cl_2, and [D$_6$]acetone were used as obtained (Cambridge Isotope Laboratories) without further purification. Chemical shifts are given in ppm relative to tms. IR spectra were recorded in the 4000–440 cm^{-1} region (step 2 cm^{-1}) on a Mattson 7000 FT-IR spectrometer with KBr pellets. Spectra for compounds **3** and **4** were measured in CH_2Cl_2 solution with ZnS cuvettes.

Synthesis of $[Mo\{\eta^4\text{-}C_5H_4(CH_2)_2\}(CO)_2(Cp)][BF_4]$ (3): A solution of **1** (0.20 g, 0.52 mmol) in CH_2Cl_2 (25 mL) was treated with excess spiro[2.4]hepta-4,6-diene (0.14 g, 1.52 mmol). After stirring the reaction mixture for 16 h, it was concentrated in vacuo to ca. 3 mL. By adding Et_2O, a yellow powder precipitated (**3**). The crude product was recrystallized from CH_2Cl_2/Et_2O and then from $CHCl_3/Et_2O$. Yield: 0.11 g (0.28 mmol, 54%). Positive-ion MS: *m*/*z* (%) = 311 $[M - BF_4]^+$, 283 $[M - BF_4 - CO]^+$, 255 $[M - BF_4 - 2(CO)]^+$, 253 (100) $[M - BF_4 - 2(CO) - H_2]^+$. ^{1}H NMR ($CD_2Cl_2$): δ = 6.37 (t, 2 H, C_5H_4), 5.81 (s, 5 H, C_5H_5), 4.80 (t, 2 H, C_5H_4), 1.35 (t, $^3J_{H,H}$ = 9 Hz, 2 H, CH_2), 0.68 (t, $^3J_{H,H}$ = 9 Hz, 2 H, CH_2) ppm. ^{13}C{^{1}H} NMR (CD_2Cl_2): δ = 225.1 (2 C, *C*O), 96.8 (2 C, C_5H_4), 94.3 (5 C, C_5H_5), 88.7 (2 C, C_5H_4), 28.6, 14.3 (2 C, CH_2) ppm. IR (CH_2Cl_2): $\tilde{\nu}$ = 2019 (s) [(ν_a(CO)], 1960 (s) [ν_s(CO)] cm^{-1}.

Synthesis of $[Mo\{\eta^4\text{-}C_5H_4(CH_2)_4\}(CO)_2(Cp)][BF_4]$ (4): The reaction was carried out as that described for compound **3**, but with spiro[4.4]nona-1,3-diene (0.18 g, 1.50 mmol). Recrystallization of the crude product was carried out with CH_2Cl_2/Et_2O. Yield: 0.19 g (0.45 mmol, 86%). Positive-ion MS: *m*/*z* (%) = 339 (100) $[M - BF_4]^+$, 311 $[M - BF_4 - CO]^+$. ^{1}H NMR (CD_2Cl_2): δ = 6.13 (t, 2 H, C_5H_4), 5.80 (s, 5 H, C_5H_5), 5.09 (t, 2 H, C_5H_4), 2.09 (t, $^3J_{H,H}$ = 7 Hz, 2 H, CH_2), 1.70 (quint, 2 H, CH_2), 1.60 (quint, 2 H, CH_2), 1.31 (t, $^3J_{H,H}$ = 7 Hz, 2 H, CH_2) ppm. ^{13}C{^{1}H} NMR (CD_2Cl_2): δ = 227.3 (2 C, *C*O), 96.4 (2 C, C_5H_4), 94.5 (5 C, C_5H_5), 85.7 (2 C, C_5H_4), 72.4 (C_{ipso}, C_5H_4) 52.3, 37.8, 25.3, 25.0 (4 C, CH_2) ppm. IR (CH_2Cl_2): $\tilde{\nu}$ = 2020 (s) [ν_a(CO)], 1964 (s) [ν_s(CO)] cm^{-1}.

Reaction of $[Mo(CO)_2(Cp)(NCCH_3)_2][BF_4]$ (1) with 1,1-Dimethyl-spiro[2.4]hepta-4,6-diene: A solution of **1** (0.20 g, 0.52 mmol) in CH_2Cl_2 (25 mL) was treated with excess 1,1-dimethyl-spiro[2.4]-hepta-4,6-diene (0.18 g, 1.50 mmol). After stirring the reaction mixture for 16 h, it was concentrated in vacuo to ca. 3 mL. By adding Et_2O, 0.14 g of an orange powder precipitated. The NMR spectrum of this product measured immediately after dissolving the product in CD_2Cl_2 shows a 1:1:1 mixture of $[Mo\{endo\text{-}\eta^4\text{-}C_5H_4CH_2C(CH_3)_2\}(CO)_2(Cp)][BF_4]$ (**7**), $[Mo\{exo\text{-}\eta^4\text{-}C_5H_4CH_2C(CH_3)_2\}(CO)_2(Cp)][BF_4]$ (**8**), and $[Mo\{\eta^5\text{-}C_5H_4C(CH_3)_2\text{-}$

CH_2-η^1-CO}(CO)(Cp)][BF_4] (**9**). The same sample measured after 12 and 24 h shows 1:2 mixture compounds **7** and **9**. **7:** ^{1}H NMR (CD_2Cl_2): δ = 6.33 (t, 2 H, C_5H_4), 5.82 (s, 5 H, C_5H_5), 4.86 (t, 2 H, C_5H_4), 1.17 (s, 2 H, CH_2), 0.90 (s, 6 H, CH_3). **8:** ^{1}H NMR (CD_2Cl_2): 6.36 (t, 2 H, C_5H_4), 5.77 (s, 5 H, C_5H_5), 4.89 (t, 2 H, C_5H_4), 1.28 (s, 6 H, CH_3), 0.48 (s, 2 H, CH_2). **9:** ^{1}H NMR (CD_2Cl_2): 6.30 (t, 2 H, C_5H_4), 5.71 (s, 5 H, C_5H_5), 5.52 (t, 2 H, C_5H_4), 2.24–2.12 (4-line m, 2 H, CH_2), 1.12 (s, 3 H, CH_3), 1.05 (s, 3 H, CH_3) ppm.

Synthesis of [Mo{η^4-$C_5H_4(CH_2)_4$}$(CO)_2$(Ind)][BF_4] (11): The reaction was carried out as that described for compound **4**, but with a solution of **2** (0.25 g, 0.57 mmol) instead of **1** in CH_2Cl_2. Recrystallization of the crude product was carried out with CH_2Cl_2/Et_2O. Yield: 0.22 g (0.53 mmol, 92%). Positive-ion MS: *m*/*z* (%) = 389 [M – BF_4]$^+$, 361 [M – BF_4 – CO]$^+$, 333 [M – BF_4 – 2(CO)]$^+$, 331 (100) [M – BF_4 – 2(CO) – H_2]$^+$, 329 [M – BF_4 – 2(CO) – 2H_2]$^+$. ^{1}H NMR ($CDCl_3$): δ = 7.78–7.75 (m, 2 H, C_9H_7), 7.41–7.37 (m, 2 H, C_9H_7), 6.37 (d, 2 H, C_9H_7), 5.74 (t, 1 H, C_9H_7), 5.30 (t, 2 H, C_5H_4), 4.85 (t, 2 H, C_5H_4), 1.83 (t, $^3J_{H,H}$ = 7 Hz, 2 H, CH_2), 1.57 (quint, 2 H, CH_2), 1.44 (quint, 2 H, CH_2), 1.10 (t, $^3J_{H,H}$ = 7 Hz, 2 H, CH_2) ppm. ^{13}C{^{1}H} NMR ($CDCl_3$): δ = 227.4 (2 C, *C*O), 130.1 (2 C, C_9H_7), 125.8 (2 C, C_9H_7), 111.9 (2C_{ipso}, C_9H_7), 95.8 (2 C, C_9H_7), 93.2 (2 C, C_5H_4), 92.4 (C_9H_7), 85.2 (2 C, C_5H_4), 71.6 (C_{ipso}, C_5H_4), 51.9, 37.1, 24.9, 24.7 (4 C, CH_2) ppm. IR (KBr): $\tilde{\nu}$ = 3102 (m), 2969 (m), 2878 (m), 2005 (vs) [ν_a(CO)], 1950 (vs) [ν_s(CO)], 1072 (br., vs) [ν(BF)] cm^{-1}. Crystals suitable for X-ray structural analysis were prepared by carefully layering the dichloromethane solution of compound **11** with a double volume of hexane.

Synthesis of [Mo(η^5-$C_5H_4CH_2$-η^1-CH_2)(CO)(Ind)][BF_4] (12): A solution of **2** (0.25 g, 0.57 mmol) in CH_2Cl_2 (25 mL) was treated with excess spiro[2.4]hepta-4,6-diene (0.14 g, 1.52 mmol). After stirring the reaction mixture for 16 h, it was concentrated in vacuo to ca. 3 mL. By adding Et_2O, an orange powder precipitated (**12**). The crude product was recrystallized from CH_2Cl_2/Et_2O. Yield: 0.23 g (0.55 mmol, 96%). Positive-ion MS: *m*/*z* (%) = 333 [M – BF_4]$^+$, 305 [M – BF_4 – CO]$^+$, 303 (100) [M – BF_4 – CO – H_2]$^+$. ^{1}H NMR (CD_2Cl_2): δ = 7.79 (d, 1 H, C_9H_7), 7.54 (t, 1 H, C_9H_7), 7.42 (t, 1 H, C_9H_7), 7.33 (d, 1 H, C_9H_7), 6.31 (d, 1 H, C_5H_4), 6.24, 6.12 (2 × s, 2 H, C_9H_7), 5.45 (t, 1 H, C_9H_7), 5.39, 4.85, 4.82 (3 × s, 3 H, C_5H_4), 2.55 (6-line m, 1 H, $C_5H_4CH_2CH_2$Mo), 2.39 (6-line m, 1 H, $C_5H_4CH_2CH_2$Mo), –0.07 (5-line m, 1 H, $C_5H_4CH_2CH_2$Mo), –3.21 (7-line m, 1 H, $C_5H_4CH_2CH_2$Mo) ppm. ^{13}C{^{1}H} NMR (CD_2Cl_2): δ = 226.4 (*C*O), 132.5, 131.6, 126.6, 124.7 (4 C, C_9H_7), 114.0, 107.9 (2C_{ipso}, C_9H_7), 97.5, 93.3, 90.7, 86.8, 86.7, 84.1, 83.3 (7 C, C_5H_4 and C_9H_7), 80.9 (C_{ipso}, C_5H_4), 19.0 ($C_5H_4CH_2CH_2$Mo), –39.3 ($C_5H_4CH_2CH_2$Mo) ppm. IR (KBr): $\tilde{\nu}$ = 3098 (m), 2947 (m), 1991 (vs) [ν(CO)], 1061 (vs) [ν(BF)] cm^{-1}. Crystals suitable for X-ray structural analysis were prepared by carefully layering the dichloromethane solution of compound **12** with a double volume of hexane.

Synthesis of [MoBr{η^5-$C_5H_4(CH_2)_2Br$}(CO)(Cp)][BF_4] (13): A solution of **12** (0.10 g, 0.24 mmol) in CH_2Cl_2 (15 mL) was cooled to –78 °C and then treated with excess bromine (0.10 g, 0.63 mmol). After stirring the mixture for 30 min at –78 °C, the volatiles were evaporated in vacuo. The crude product was recrystallized from CH_2Cl_2/Et_2O to obtain **13** as a purple powder. Yield: 0.13 g (0.22 mmol, 94%). Positive-ion MS: *m*/*z* (%) = 493 [M – BF_4]$^+$, 465 (100) [M – BF_4 – CO]$^+$, 384 [M – BF_4 – CO – Br]$^+$. ^{1}H NMR ([D_6]-acetone): δ = 8.02 (d, 1 H, C_9H_7), 7.84–7.76 (m, 2 H, C_9H_7), 7.60 (d, 1 H, C_9H_7), 6.69 (t, 1 H, C_9H_7), 6.47 (d, 2 H, C_9H_7), 6.35 (t, 1 H, C_5H_4), 6.27 (t, 1 H, C_5H_4), 6.22 (q, 1 H, C_5H_4), 6.03 (q, 1 H, C_5H_4), 3.54 (6-line m, 2 H, $C_5H_4CH_2CH_2$Br), 2.76 (t, 2 H, $C_5H_4CH_2CH_2$Br) ppm. ^{13}C NMR ([D_6]acetone): δ = 218.3 (*C*O), 135.7, 135.6, 130.9, 128.7 (4 C, C_9H_7), 121.6, 121.5 (2C_{ipso}, C_9H_7), 112.8 (C_{ipso}, C_5H_4), 106.2, 102.3, 99.2, 94.4, 91.1, 91.0, 87.3 (7 C, C_5H_4 and C_9H_7), 33.3, 32.9 (2 C, CH_2) ppm. IR (KBr): $\tilde{\nu}$ = 3138 (m), 3109 (m), 3097 (m), 3063 (m), 2055 (vs) [ν(CO)], 1062 (vs) [ν(BF)] cm^{-1}.

Synthesis of [MoBr{η^5-$C_5H_4(CH_2)_2Br$}(CO)(Ind)][Br]·0.5H_2O (13a): The reaction was carried out as that described for compound **13**, but at room temperature. The crude product was recrystallized several times from CH_2Cl_2/ether and acetone/ether. Crystals suitable for X-ray structural analysis were prepared by carefully layering the dichloromethane solution of compound **13a** with a double volume of hexane.

Synthesis of [Mo{η^5-$C_5H_4(CH_2)_2I$}(CO)(Cp)I][BF_4] (14): A solution of **12** (0.10 g, 0.24 mmol) in CH_2Cl_2 (15 mL) was cooled to –78 °C and then treated with excess iodine (0.14 g, 0.59 mmol). After stirring the mixture for 30 min at –78 °C, the volatiles were evaporated in vacuo. The crude product was washed with Et_2O and then recrystallized from CH_2Cl_2/Et_2O to obtain **14** as a purple powder. Yield: 0.15 g (0.22 mmol, 93%). Positive-ion MS: *m*/*z* (%) = 587 (100) [M – BF_4]$^+$, 559 [M – BF_4 – CO]$^+$. ^{1}H NMR ([D_6]-acetone): δ = 7.94–7.89 (m, 2 H, C_9H_7), 7.76 (d, 1 H, C_9H_7), 7.63 (t, 1 H, C_9H_7), 6.68 (s, 2 H, C_9H_7), 6.63 (s, 2 H, C_9H_7), 6.44 (t, 1 H, C_9H_7), 6.37 (s, 1 H, C_5H_4), 6.28 (s, 1 H, C_5H_4), 6.23 (s, 1 H, C_5H_4), 6.13 (s, 1 H, C_5H_4), 3.37 (6-line m, 2 H, $C_5H_4CH_2CH_2$I), 2.84 (6-line m, 2 H, $C_5H_4CH_2CH_2$I) ppm. ^{13}C NMR ([D_6]acetone): δ = 219.3 (*C*O), 135.4, 135.1, 132.4, 128.3 (4 C, C_9H_7), 117.9, 117.0 (2C_{ipso}, C_9H_7), 112.4 (C_{ipso}, C_5H_4), 103.3, 101.7, 98.1, 96.4, 91.0, 90.0, 86.9 (7 C, C_5H_4 and C_9H_7), 34.5 ($C_5H_4CH_2CH_2$I), 4.7 ($C_5H_4CH_2CH_2$I) ppm. IR (KBr): $\tilde{\nu}$ = 3127 (m), 3086 (m), 2049 (vs) [ν(CO)], 1057 (vs) [ν(BF)] cm^{-1}.

X-ray Crystallography: Suitable single-crystals of **11**, **12**, and **13a** were manually harvested from the crystallization vials and mounted on a Hampton Research CryoLoops by using FOMBLIN Y perfluoropolyether vacuum oil (LVAC 25/6) purchased from Aldrich,[36] with the help of a Stemi 2000 stereomicroscope equipped with Carl Zeiss lenses. Data were collected on a Bruker X8 Kappa APEX II charge-coupled device (CCD) area-detector diffractometer (Mo-K_α graphite-monochromated radiation, λ = 0.7107 Å) controlled by the APEX2 software package[37] and equipped with an Oxford Cryosystems Series 700 cryostream that is monitored remotely by the software interface Cryopad.[38] Images were processed by using the software package SAINT+,[39] and data were corrected for absorption by the multiscan, semi-empirical method implemented in SADABS.[40] The structures were solved by using Patterson synthesis with SHELXS-97,[41] which allowed the immediate location of the central molybdenum metallic center for each complex and the Br atoms in compound **13a**. All the remaining non-hydrogen atoms were directly located with difference Fourier maps calculated from successive full-matrix, least-squares refinement cycles on F^2 by using SHELXL-97.[42] All non-hydrogen atoms were successfully refined by using anisotropic displacement parameters. Hydrogen atoms attached to carbon were located at their idealized positions with appropriate *HFIX* instructions in SHELXL: *43* for the aromatic hydrogen atoms associated with the Cp-substituted rings and indenyl molecules; *13* and *23* for the hydrogen atoms associated with the conjugated diene of spiro[4.4]-nona-1,3-diene and the –CH_2– chains, respectively. These hydrogen atoms were included in subsequent refinement cycles in riding-motion approximation with isotropic thermal displacements parameters (U_{iso}) fixed at 1.2 times U_{eq} of the carbon atom to which they are attached.

Table 5. Crystal and structure refinement data for [Mo{η⁴-$C_5H_4(CH_2)_4$}(CO)$_2$(Ind)][BF_4] (**11**), [Mo(η⁵-$C_5H_4CH_2$-η¹-CH_2)(CO)(Ind)][BF_4] (**12**) and [MoBr{η⁵-$C_5H_4(CH_2)_2$Br}(CO)(Ind)][Br]·0.5H_2O (**13a**).

	11	**12**	**13a**
Formula	$C_{20}H_{19}BF_4MoO_2$	$C_{34}H_{30}B_2F_8Mo_2O_2$	$C_{34}H_{32}Br_6Mo_2O_3$
Formula weight	474.10	836.08	1159.94
Temperature [K]	100(2)	150(2)	150(2)
Crystal system	triclinic	monoclinic	triclinic
Space group	$P\bar{1}$	$P2_1/c$	$P\bar{1}$
a [Å]	7.4845(7)	15.2570(5)	7.9201(2)
b [Å]	7.6375(8)	8.5965(3)	13.5129(4)
c [Å]	16.6146(17)	24.2930(9)	18.0301(4)
α [°]	80.378(5)	–	72.2750(10)
β [°]	82.324(5)	96.837(2)	81.8240(10)
γ [°]	78.153(5)	–	73.2650(10)
Volume [Å^3]	911.57(16)	3163.53(19)	1757.05(8)
Z	2	4	2
Z'	–	2	2
D_c [g cm^{-3}]	1.727	1.755	2.192
μ(Mo-K_α) [mm^{-1}]	0.772	0.872	7.570
F(000)	476	1664	1108
Crystal size [mm]	0.22 × 0.16 × 0.04	0.40 × 0.24 × 0.16	0.36 × 0.25 × 0.16
Crystal type	red blocks	red blocks	red blocks
θ range	3.52 to 27.48	3.59 to 31.63	3.57 to 27.48
Index ranges	$-9 \le h \le 9$	$-22 \le h \le 22$	$-10 \le h \le 10$
	$-9 \le k \le 9$	$-12 \le k \le 12$	$-17 \le k \le 17$
	$-21 \le l \le 21$	$-35 \le l \le 35$	$-21 \le l \le 23$
Reflections collected	38877	124636	53608
Independent reflections	4135	10596	7997
	(R_{int} = 0.0313)	(R_{int} = 0.0394)	(R_{int} = 0.0421)
Data completeness [%]	99.0	99.6%	99.2%
Parameters	253	491	412
Final R indices [$I > 2\sigma(I)$][a,b]	R_1 = 0.0479	R_1 = 0.0477	R_1 = 0.0284
	wR_2 = 0.1257	wR_2 = 0.1164	wR_2 = 0.0573
Final R indices (all data)[a,b]	R_1 = 0.0522	R_1 = 0.0641	R_1 = 0.0426
	wR_2 = 0.1283	wR_2 = 0.1270	wR_2 = 0.0607
Weighting scheme[c]	m = 0.0536	m = 0.0548	m = 0.0173
	n = 4.0207	n = 8.2897	n = 3.9398
Largest diff. peak and hole [e Å^{-3}]	2.462, –1.140	4.016, –1.414	1.070, –0.713

[a] $R_1 = \Sigma||F_o| - |F_c||/\Sigma|F_o|$. [b] $wR_2 = \{\Sigma[w(F_o^2 - F_c^2)^2]/\Sigma[w(F_o^2)^2]\}^{1/2}$. [c] $w = 1/[\sigma^2(F_o^2) + (mP)^2 + nP]$ where $P = (F_o^2 + 2F_c^2)/3$.

In structure **12**, the two BF_4^- anions were found to be statistically disordered over two distinct crystallographic positions. This statistical disorder was modeled for the two anions over a central and common to the two positions B–F bond with fixed rates of occupancy of 0.80:0.20 and 0.70:0.30. Moreover, in order to ensure chemically reasonable geometries for these moieties, the B–F and F···F distances of all moieties were restrained to common (but refinable) values, which ultimately refined to 1.356(1) and 2.210(1) Å, respectively.

In structure **13a**, the two hydrogen atoms associated with the water molecule of crystallization were markedly visible from the last difference Fourier map synthesis, and were included in the final structural model, with the O–H and H···H distances restrained to 0.95(1) and 1.55(1) Å (in order to ensure a chemically reasonable geometry for this moiety) and by using a riding model with an isotropic displacement parameter fixed at *1.5* times U_{eq} of the oxygen atom to which they are attached.

The last difference Fourier map synthesis showed, for **11**, the highest peak (2.462 e Å^{-3}) and deepest hole (–1.140 e Å^{-3}) located at 1.77 Å from F(2) and 0.74 Å from Mo(1), respectively; for **12**, the highest peak (4.016 e Å^{-3}) and deepest hole (–1.414 e Å^{-3}) are located at 0.70 Å from Mo(1) and 0.61 Å from Mo(2), respectively; for **13a**, the highest peak (1.070 e Å^{-3}) and deepest hole (–0.713 e Å^{-3}) are instead located at 0.94 Å from Br(6) and 0.89 Å from Mo(2), respectively. Crystallographic data and structure refinement details are summarized in Table 5.

CCDC-634114, CCDC-634115 and CCDC-634116 (for **11**, **12** and **13a**) contain the supplementary crystallographic data for this paper. These data can be obtained free of charge from The Cambridge Crystallographic Data Centre via www.ccdc.cam.ac.uk/data_request/cif.

Supporting Information (see footnote on the first page of this article): The composition of the compounds prepared was checked by mass spectrometry and NMR spectroscopy. Positive-ion electrospray ionization (ESI) mass spectra and $^{13}C\{^1H\}$ NMR spectra are included.

Acknowledgments

We are grateful to *Fundação para a Ciência e Tecnologia* (FCT, Portugal) for supporting the postdoctoral project SFRH/BPD/24889/2005 and for funding the purchase of the single-crystal diffractometer. We wish to acknowledge Ana Varela Coelho for providing data from the Mass Spectrometry Service at the Instituto de Tecnologia Química e Biológica, Universidade Nova de Lisboa, Oeiras, Portugal.

[1] H. Köpf, P. Köpf-Maier, *Angew. Chem. Int. Ed. Engl.* **1979**, *18*, 477–478.
[2] J. B. Waern, P. Turner, M. M. Harding, *Organometallics* **2006**, *25*, 3417–3421.
[3] J. Vinklárek, H. Paláčková, J. Honzíček, J. Holubová, M. Holčapek, I. Císařova, *Inorg. Chem.* **2006**, *45*, 2156–2162.
[4] a) P. Ghosh, A. T. Kotchevar, D. D. DuMez, S. Ghosh, J. Peiterson, F. M. Uckun, *Inorg. Chem.* **1999**, *38*, 3730–3737; b) P. Ghosh, S. Ghosh, C. Navara, R. K. Narla, A. Benyumov, F. M. Uckun, *J. Inorg. Biochem.* **2001**, *84*, 241–253.
[5] a) J. Wald, R. Alberto, K. Ortner, L. Candreia, *Angew. Chem. Int. Ed.* **2001**, *40*, 3062–3066; b) R. Schibli, P. A. Schubiger, *Eur. J. Nucl. Med.* **2002**, *29*, 1529–1542.
[6] a) O. R. Allen, L. Croll, A. L. Gott, R. J. Knox, P. C. McGowan, *Organometallics* **2004**, *23*, 288–292; b) P. W. Causey, M. C. Baird, S. P. C. Cole, *Organometallics* **2004**, *23*, 4486–4494.
[7] A. Gansäuer, D. Franke, T. Lauterbach, M. Nieger, *J. Am. Chem. Soc.* **2005**, *127*, 11622–11623.
[8] Y. Qian, J. Huang, M. D. Bala, B. Lian, H. Zhang, H. Zhang, *Chem. Rev.* **2003**, *103*, 2633–2690.
[9] a) J. R. Boyles, M. C. Baird, B. G. Campling, N. Jain, *J. Inorg. Biochem.* **2001**, *84*, 159–162; b) M. Tacke, L. P. Cuffe, W. M. Gallagher, Y. Lou, O. Mendoza, H. Müller-Bunz, F.-J. K. Rehmann, N. Sweeney, *J. Inorg. Biochem.* **2004**, *98*, 1987–1994.
[10] M. C. Valadares, A. L. Ramos, F.-J. K. Rehmann, N. J. Sweeney, K. Strohfeldt, M. Tacke, M. L. S. Queiroz, *Eur. J. Pharmacol.* **2006**, *534*, 264–270.
[11] a) J. B. Waern, M. M. Harding, *J. Organomet. Chem.* **2004**, *689*, 4655–4668; b) A. Erxleben, *Inorg. Chem.* **2005**, *44*, 1082–1094; c) J. B. Waern, M. M. Harding, *Inorg. Chem.* **2004**, *43*, 206–213; d) J. L. Vera, F. R. Román, E. Meléndez, *Bioorg. Med. Chem.* **2006**, *14*, 8683–8691.
[12] a) J. R. Ascenso, C. G. Deazevedo, I. S. Gonçalves, E. Herdtweck, D. S. Moreno, M. Pessanha, C. C. Romão, *Organometallics* **1995**, *14*, 3901–3919; b) I. S. Gonçalves, E. Herdtweck, C. C. Romão, B. Royo, *J. Organomet. Chem.* **1999**, *580*, 169–177; c) T. C. Forschner, J. A. Carella II, N. J. Cooper, *Organometallics* **1989**, *9*, 2478–2483; d) T. C. Forschner, N. J. Cooper, *J. Am. Chem. Soc.* **1989**, *111*, 7420–7424; e) R. P. Hughes, S. M. Maddock, I. A. Guzei, L. M. Liable-Sands, A. L. Rheingold, *J. Am. Chem. Soc.* **2001**, *123*, 3279–3288.
[13] a) J. H. Shin, W. Savage, V. J. Murphy, J. B. Bonanno, D. G. Churchill, G. Parkin, *J. Chem. Soc., Dalton Trans.* **2001**, 1732–1753; b) J. C. Green, M. L. H. Green, C. P. Morley, *J. Organomet. Chem.* **1982**, *233*, C4–C6; c) L. Labella, A. Chernega, M. L. H. Green, *J. Chem. Soc., Dalton Trans.* **1995**, 395–402.
[14] a) A. Barretta, F. G. N. Cloke, A. Feigenbaum, M. L. H. Green, A. Gourdon, K. Prout, *J. Chem. Soc., Chem. Commun.* **1981**, 156–158; b) F. Amor, P. Royo, T. P. Spaniol, J. Okuda, *J. Organomet. Chem.* **2000**, *604*, 126–131.
[15] A. Barretta, K. S. Chong, F. G. N. Cloke, A. Feigenbaum, M. L. H. Green, *J. Chem. Soc., Dalton Trans.* **1983**, 861–864.
[16] C. G. Kreiter, M. Wenz, P. Bell, *J. Organomet. Chem.* **1990**, *394*, 195–211.
[17] P. Eilbracht, *Chem. Ber.* **1976**, *109*, 1429–1435.
[18] a) M. Bottrill, M. Green, *J. Chem. Soc., Dalton Trans.* **1977**, 2365–2371; b) J. R. Ascenso, C. G. Deazevedo, I. S. Gonçalves, E. Herdtweck, D. S. Moreno, C. C. Romão, J. Zühlke, *Organometallics* **1994**, *13*, 429–431; c) I. S. Gonçalves, C. C. Romão, *J. Organomet. Chem.* **1995**, *486*, 155–161.
[19] a) P. Eilbracht, P. Dahler, *J. Organomet. Chem.* **1977**, *127*, C48–C50; b) P. Eilbracht, U. Mayser, *Chem. Ber.* **1980**, *113*, 2211–2220; c) P. Eilbracht, P. Dahler, G. Tiedtke, *J. Organomet. Chem.* **1980**, *185*, C25–C28; d) P. Eilbracht, *Chem. Ber.* **1976**, *109*, 3136–3141.
[20] Y. T. Fu, P. C. Chao, L. K. Liu, *Organometallics* **1998**, *17*, 221–226.
[21] a) H. Müller, G. E. Herberich, *Chem. Ber.* **1971**, *104*, 2772–2780; b) H. Müller, G. E. Herberich, *Chem. Ber.* **1971**, *104*, 2780–2785.
[22] a) F. H. Allen, *Acta Crystallogr., Sect. B* **2002**, *58*, 380–388; b) F. H. Allen, W. D. S. Motherwell, *Acta Crystallogr., Sect. B* **2002**, *58*, 407–422.
[23] J. W. Faller, R. H. Crabtree, A. Habib, *Organometallics* **1985**, *4*, 929–935.
[24] L. A. Paquette, G. A. Odoherty, B. L. Miller, R. D. Rogers, A. L. Rheingold, S. L. Geib, *Organometallics* **1989**, *8*, 2167–2172.
[25] a) A. Gourdon, K. Prout, *Acta Crystallogr. Acta Crystallogr., Sect. B* **1981**, *37*, 1982–1985; b) W. Frank, C. G. Kreiter, G. J. Reiss, S. Schufft, *Acta Crystallogr., Sect. C* **1996**, *52*, 356–358.
[26] J. C. Green, M. L. H. Green, C. P. Morley, *J. Organomet. Chem.* **1982**, *233*, C4–C6.
[27] a) K. W. Barnett, *Inorg. Chem.* **1969**, *8*, 2009–2011; b) O. G. Adeyemi, N. J. Coville, *Organometallics* **2003**, *22*, 2284–2290.
[28] P. Eilbracht, W. Fassmann, W. Diehl, *Chem. Ber.* **1985**, *118*, 2314–2329.
[29] S. W. Staley, J. J. Rocchio, *J. Am. Chem. Soc.* **1969**, *91*, 1565–1566.
[30] J. Zhao, E. Herdtweck, F. E. Kuehn, *J. Organomet. Chem.* **2006**, *691*, 2199–2206.
[31] W. L. F. Armarego, D. D. Perrin, *Purification of Laboratory Chemicals*, Butterworth-Heinemann, Oxford, **1996**.
[32] M. L. H. Green, D. Ohare, *J. Chem. Soc., Dalton Trans.* **1985**, 1585–1590.
[33] I. Erden, F. P. Xu, A. Sadoun, W. Smith, G. Sheff, M. Ossun, *J. Org. Chem.* **1995**, *60*, 813–820.
[34] C. C. L. Pereira, S. S. Braga, F. A. A. Paz, M. Pillinger, J. Klinowski, I. S. Gonçalves, *Eur. J. Inorg. Chem.* **2006**, 4278–4288.
[35] R. D. Vocke, *Pure Appl. Chem.* **1999**, *71*, 1593–1607.
[36] T. Kottke, D. Stalke, *J. Appl. Crystallogr.* **1993**, *26*, 615–619.
[37] *APEX2*, *Data Collection Software Version 2.1-RC13*, Bruker AXS, Delft, The Netherlands, **2006**.
[38] *Cryopad*, *Remote Monitoring and Control, Version 1.451*, Oxford Cryosystems, Oxford, United Kingdom, **2006**.
[39] *SAINT+, Data Integration Engine Version 7.23a* © **1997–2005**, Bruker AXS, Madison, Wisconsin, USA.
[40] G. M. Sheldrick, *SADABS Version 2.01*, *Bruker/Siemens Area Detector Absorption Correction Program*, Bruker AXS, Madison, Wisconsin, USA, **1998**.
[41] G. M. Sheldrick, *SHELXS-97, Program for Crystal Structure Solution*, University of Göttingen, **1997**.
[42] G. M. Sheldrick, *SHELXL-97, Program for Crystal Structure Refinement*, University of Göttingen, **1997**.

Received: January 29, 2007
Published Online: May 10, 2007

